AZT Binding to DNA and RNA: Molecular Modeling and Biological Significance

H.A. Tajmir-Riahi

*Department of Chemistry-Biology, University of Québec at Trois-Rivières, C.P. 500,
(Québec) Canada G9A 5H7*

In this review we report the application of molecular modeling based on different analytical methods to locate the binding sites of anti-AIDS drug azidothymidine (AZT) in the major and minor grooves of DNA and RNA duplexes. The effects of drug complexation on nucleic acids secondary structures and the biological implication are discussed.

INTRODUCTION

Studies have shown primer unblocking and rescue of DNA synthesis AZT-resistant HIV-1 reverse transcriptase on DNA and RNA templates [1]. AZT (Structure 1), a nucleobase reverse transcriptase inhibitor, was the first drug approved by Food and Drug Administration (FDA) for the treatment of AIDS and is still widely used in combination with other antiviral drugs [2]. The use of highly active antiretroviral drugs against HIV-1 virus dramatically decreased the mortality related to AIDS in developed countries [3]. Highly active antiretroviral treatments usually combine inhibitors of the viral protease, that is required for maturation of the viral particles, with inhibitor of reverse transcriptase which converts single stranded RNA to DNA [2]. A recent report shows the primer unblocking and rescue of DNA synthesis by AZT-resistant HIV-1reverse transcriptase [1]. On the other hand, oxidative DNA damage has been reported in fetal tissues by

**AZT
Structure 1**
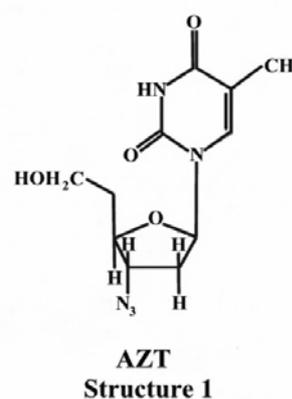
exposure to AZT [4,5]. It has been shown that skin tumors initiated in mouse fetuses by AZT to have a major incidence of G→A and G→T mutations in codons 12 and 13 of H-*ras* oncogene [6]. Oxidative DNA damage is plausible, since mitochondria have been found to be the cellular targets for AZT, resulting in ultrastructural, biochemical and molecular

___
* Corresponding author. E-mail: tajmirri@uqtr.ca

abnormalities [7]. Significant increases in 8-oxo-2′-deoxyguanosine (8-oxo-dG) were also found in the livers, a target tissue for transplacental carcinogenesis, and in kidneys [4]. Genotoxic and carcinogenic effects of AZT have been shown *in vivo* and *in vitro* [8]. Experiments performed in cultured cells demonstrated preferential AZT incorporation into telomeric DNA of cells containing an active telomerase [9,10]. We have recently shown the binding of AZT to G-C, A-T bases and the backbone phosphate group of DNA duplex with partial B to A-DNA conformational changes.

This review reports the results of molecular modeling for AZT-DNA and AZT-RNA complexes based on capillary electrophoresis, FTIR and UV-visible spectroscopic methods.

EXPERIMENTAL

Materials

Yeast Baker tRNA sodium salt was purchased from Sigma Chemical Co., and used as supplied. AZT was obtained from Sigma Chemical Company. Other chemicals were of reagent grade and used without further purification.

Preparation of Stock Solutions

Sodium-RNA or sodium-DNA was dissolved to 1% (w/w) (0.025 M nucleotide/phosphate) in 0.1 M NaCl and 1 mM sodium cacodylate (pH 7.30) at 5 °C for 24 h with occasional stirring to ensure the formation of a homogeneous solution. The appropriate amount of AZT (0.3 to 25 mM) was prepared in water. The drug solution was then added dropwise to RNA or DNA solution to attain desired AZT/polynucleotide (P) molar ratios of 1/80, 1/40, 1/20, 1/10, 1/4 and 1/2 at a final DNA or RNA concentration of 0.5% (w/w) or 12.5 mM (phosphate) for infrared measurements, and 1/800 to 1/3 with final DNA or RNA content of 1.25 mM (phosphate) for capillary electrophoresis. The pH of the solutions was adjusted to 6.5-7.5 with pH meter ORION model 210A, using NaOH solution. The infrared spectra were recorded 2 h after incubation of drug with polynucleotide solutions.

Absorption Spectroscopy

The absorption spectra were recorded on a Perkin Elmer Lamda 40 spectrophotometer, using various AZT concentrations (1 μM to 1 mM) and RNA or DNA concentration of 0.1 mM.

FTIR Spectroscopy

Infrared spectra were recorded on a Bomem DA3-0.02 FTIR spectrometer equipped with a nitrogen cooled HgCdTe detector and KBr beam splitter. The solution spectra are taken using AgBr windows with resolution of 4 cm^{-1} and 100-500 scans. Each set of infrared spectra was taken (three measurements) on three identical samples with the same RNA or DNA and drug concentrations. The water subtraction was carried out with 0.1 M NaCl solution used as a reference at pH 6.5-7.5 [11]. A good water subtraction is achieved as shown by a flat baseline around 2200 cm^{-1}, where the water combination mode is located. This method is a rough estimate, but removes the water content in a satisfactory way [11]. The difference spectra [(polynucleotide solution + AZT solution)-(polynucleotide solution)] are produced, using a sharp RNA band at 861 and DNA band at 966 cm^{-1} as internal references. This band, due to sugar C-C and C-O stretching vibrations, exhibited no spectral changes (shifting or intensity variations) on drug complexation and was cancelled upon spectral subtraction. The intensity ratios of several RNA and DNA in-plane vibrations related to A-T, A-U and G-C bases and the PO$_2$ stretching are measured with respect to the reference bands as a function of AZT concentrations with an error of ±3%.

Capillary Eectrophoresis

A P/ACE System MDQ (Beckman) with photodiode array detector was used to study AZT-RNA and AZT-DNA interactions. Uncoated fused silica capillary of 75 μm i.d. and effective length of 50 cm was used. The capillary was initially conditioned by washing with 1 N sodium hydroxide for 30 min, followed by a 15-min wash with 0.1 M sodium hydroxide. Then it was extensively rinsed with deionized water and running buffer before use. Samples were injected using voltage injection at 10 kV for 5 s. Electrophoresis was carried out at a voltage of 25 kV for 10 min, using normal polarity and all runs were carried out at 25 °C. The electropherograms were monitored at 260 nm in a run buffer containing 20 mM Tris-HCl pH 7.0 ± 0.2. The capillary inlet and outlet vials were replenished after every 5 runs.

Experiments for bindings of AZT to RNA and to DNA

were performed in a sample buffer containing 20 mM Tris-HCl pH 7.0 ± 0.2, using constant concentration of yeast tRNA or calf-thymus DNA (1.25 mM) and variable concentrations of AZT. The stock solutions of 2.5 mM of AZT and 2.5 mM of RNA or DNA were prepared in the sample buffer. The solutions were mixed to attain AZT/nucleotide (P) molar ratios of 1/800 to 1/6 in the presence of 1.25 mM of nucleotide(phosphate). The data analysis was carried out according to our recent report [12].

Molecular Modeling

Molecular modeling study was carried out based on simple molecular dynamics simulations of the ligand-RNA and ligand-DNA complexes. All of the calculations described below were performed using HyperChem 7.0 software [13]. Modeling of RNA and DNA Duplex and AZT Structure. To build a model of a RNA- or DNA-ligand molecular complex, the A-form RNA decamer 5'-r(GpCpApUpCpGpUpApGpC)-3' and B-form DNA d(GpCpApUpCpGpUpApGpC)-3' was constructed using HyperChem Nucleic acids Databases. The choice of this particular model of RNA or DNA was based on the fact that AZT molecule has slightly higher binding affinities for the GC bases compared to the A-T bases Model for the AZT molecule was built manually using drawing tools of the HyperChem Model Builder. First, the AZT molecules was "sketched" in two dimensions (2D) and then converted into three dimensional (3D) entities using 2D to 3D conversion tool in the HyperChem Model Builder.

Docking Studies

Docking of AZT molecule into the minor groove of RNA or DNA duplex was carried out manually as follows: we moved the AZT molecule to an initial position that approximates the formation of a hydrogen and/or covalent bonds between -NH/-OH atoms of AZT and N3/N2-H atoms of guanine and O2 atom of uracil or thymine. Indeed, the main reactive sites for guanine and uracil bases in the A-form RNA are N3/N2-H and O2, respectively. The next step was to minimize the AZT structure by performing a molecular mechanics optimization using AMBER force field [14]. After AZT is optimized the complex was then subjected to energy minimization until full convergence (energy gradient ≤ 0.01 kcal mol^{-1} Å^{-1}) was reached. These simple calculations proved

effective in locating potential ligand binding sites.

Molecular Dynamics Simulations

Molecular Dynamics was performed to obtain a lower energy minimum for the ligand-RNA and ligand-DNA complexes. All calculations were performed in the AMBER force field [14], using standard parameters. The following protocol was used to carry out the molecular dynamics studies: The simulations were performed for 10 picoseconds (ps) using heat time of 0.1 ps and temperature step of 30 K. Because the gradient is very small in the starting system (corresponding to a near-zero temperature), a short heat time of 0.1 ps is used to raise the temperature from a starting temperature of 10 K to the simulation temperature of 300 K incrementing by temperature step of 30 K. Since no periodic boundary conditions were imposed, we have modelled the RNA-AZT system in the solution. A distance-dependent dielectric constant was applied to simulate electrostatic screening since explicit water was not included. This simulation was performed for considerably simplified system with a rigid structure of RNA or DNA, thus only the ligand could be moved. During simulations, all of the intermittent structures of the complexes formed at every successive 0.5 ps were saved and then were subjected to energy minimization. The minima obtained for each complex were screened to identify the lowest energy minimum, and that was taken as a representative of energetically favorable complex. Energy of interaction (E_{int}) between RNA or DNA and AZT molecule in a complex was calculated as follows:

$$E_{int} = E_{complex} - (E_{RNA} + E_{AZT})$$

where E_{int} = energy of interaction of a complex, $E_{complex}$ = total energy of the complex and E_{RNA} and E_{AZT} are the individual total energies of the RNA or DNA and AZT molecules calculated after they are separated from each other [15].

RESULTS and DISCUSSION

FTIR Spectra of AZT-RNA and AZT-DNA Complexes

AZT-RNA adducts. No major AZT-RNA interaction was observed at low drug concentrations (1/80 and 1/40). Evidence

for this comes from no major spectral changes (intensity or shifting) of several polynucleotides in-plane vibrations related to the G-C, A-U bases and the backbone phosphate modes at 1698 (mainly G), 1653 (mainly U), 1608 (A), 1488 (mainly C) and 1244 cm^{-1} (asymmetric PO_2 stretching vibration) [11,12, 16-20], in the presence of AZT [21].

As drug concentration increased (r = 1/20 to 1/2), increases in the intensities of the bands at 1698 (guanine) and 1653 cm^{-1} (uracil) were observed [21]. These intensity variations of RNA vibrational frequencies were also associated with the shifting of the bands at 1698 (G) to 1694 cm^{-1}, 1653 (U) to 1661 cm^{-1} and 1244 (PO_2) to 1250 cm^{-1}, upon AZT complexation. However, minor intensity increase was observed for the PO_2 band at 1244 cm^{-1}. The observed spectral changes are indicative of major AZT bindings to the guanine and uracil bases with minor perturbations of the backbone PO_2 group (due to the lack of major intensity variations of the phosphate band at 1244 cm^{-1}). It is worth mentioning that the several positive features centered at 1697, 1472, 1273 and 1102 cm^{-1}, in the difference spectra of drug-RNA complexes are arising from the AZT vibrational frequencies and they are not due to RNA vibrations [21]. The bands at 1608 (mainly A) and 1488 cm^{-1} (mainly C) showed no intensity changes upon drug interaction. However, the adenine band at 1608 cm^{-1} shifted towards a lower frequency at 1602 cm^{-1} upon drug interaction.

The observed spectral changes are indicative of no drug interaction with cytosine bases, while a weak interaction between AZT and adenine base can not be excluded. Similar infrared spectral changes were observed for other AZT-DNA complexes, where drug bindings to G-C and A-T base pairs were observed [21].

AZT-DNA adducts. At low AZT concentration (r =1/80), no drug-DNA interaction occurs. Evidence for this comes from no major spectral changes (intensity or shifting) of several polynucleotides in-plane vibrations related to the G-C, A-T bases and the backbone phosphate modes at 1717 (mainly G), 1663 (mainly T), 1609 (A), 1492 (mainly C) and 1222 cm^{-1} (asymmetric PO_2 stretching vibration) [11,16-20] in the presence of AZT [22].

As drug concentration increases (r > 1/40), an increase in the intensities of the bands at 1717 (guanine) 1663 (thymine), and 1222 cm^{-1} (phosphate) is observed. This increase in intensity of DNA in-plane vibrations was characterized by

positive features at 1720 (G), 1660 (T) and 1214 (PO_2) and 1080 cm^{-1} (PO_2) in the difference spectra of the AZT-DNA complexes. It is worth mentioning, that the other positive features centered at 1480 and 1270 cm-1 in the difference spectra of drug-DNA complexes are caused by the AZT vibrational frequencies and are not due to DNA vibrations [22]. These intensity variations of DNA vibrational frequencies were also associated with the shifting of the bands at 1707 (G) to 1713; 1663 (T) to 1666 and 1222 (PO_2) to 1225 cm^{-1}, upon AZT complexation. The observed spectral changes are indicative of major AZT bindings to the guanine, thymine bases and the backbone PO_2 groups. The bands at 1609 (A) and 1492 cm^{-1} (mainly C) showed no intensity changes upon drug interaction. However, the adenine band at 1609 shifted towards a lower frequency at 1602 cm^{-1} upon drug interaction. The observed spectral changes are indicative of no drug complexation with cytosine bases, while AZT-adenine interaction can not be excluded [22].

The increase in intensities of the bands at 1717 (G), 1663 (T) and 1222 cm^{-1} (PO_2) continued up to r = 1/10, indicating major AZT interaction with guanine, thymine and backbone phosphate groups. Similar infrared spectral changes were observed for the other drug-DNA complexes. At high drug concentration r => 10, minor decrease of intensities were observed for the band at 1717 (G), 1663 (T) and 1222 cm^{-1} (PO_2), due to DNA aggregation in the presence of AZT in aqueous solution. Similar decrease of intensity was observed for the DNA in-plan vibrations, when DNA aggregation occurred in the presence of chlorophyll at high pigment concentration [23].

Additional evidence regarding AZT-RNA complexation comes also from the major shift of drug vibrational frequencies. A strong band at 1690 cm^{-1} related to the drug C=O and C=C stretchings [23], was shifted to 1697 cm^{-1}, in the spectra of AZT-RNA and DNA complexes [21,22]. The observed spectral changes are indicative of AZT-polynucleotide interaction through drug polar groups.

RNA and DNA conformations. The AZT-RNA interaction leads to no major RNA secondary structural changes. The marker infrared bands for RNA in A-conformation were located at 1698 (G), 1244 (phosphate), 861 (ribose-phosphate) and 810 cm^{-1} (ribose-phosphate) in the spectrum of the free RNA [18,20,24]. These vibrations

exhibited no major shifting upon AZT complexation and, therefore, RNA remains in the A-conformation in the AZT-RNA adducts [21].

The AZT-DNA interaction leads to a partial B to A-DNA conformational transition. Evidence for this comes from the shift of the B-DNA marker bands at 1717 (G), 1222 (PO_2) and 836 cm^{-1} (phosphodiester mode) [18,20,24], in the spectra of the AZT-DNA complexes. When B to A transition occurs, the DNA marker bands are shifted to 1710-1700 cm^{-1}, 1225-1240 cm^{-1} and 825-800 cm^{-1} respectively and a new band appears at about 870-860 cm^{-1} [18,20,24]. In the B to Z conformational transition, the sugar-phosphate band at 836 cm^{-1} appears at 800-780 cm^{-1} and the guanine band displaces to 1690 cm^{-1}, while the phosphate band shifts to 1216 cm^{-1} [18,20,24]. Upon AZT-DNA complexation, the band at 1717 shifted to 1707 cm^{-1}, the phosphate band at 1222 appeared at 1225 cm^{-1} and the phosphodiester band at 836 lost intensity and a new band emerged at 810 cm^{-1} [22]. The observed spectral changes for DNA marked bands showed a partial B to A-DNA conformational transition upon AZT interaction [22].

The furanose ring in the free AZT moiety shows C2′-endo/anti with marker infrared bands at 892 and 840 cm^{-1}, which is suggested to be a preferred conformation for AZT interaction with HIV-1 [23]. Since no major shifting of these vibrations occurred and no new bands were observed in the region of 900-800 cm^{-1}, the sugar moiety of AZT remains in the C2′-endo/anti pucker, in these AZT-RNA and AZT-DNA adducts [21,22].

Capillary Electrophoresis of AZT-RNA and AZT-DNA Complexes

Additional evidence regarding AZT-RNA and AZT-DNA complexation comes from capillary electrophoresis. Reaction mixtures containing constant amount of RNA or DNA (1.25 mM) and various amounts of AZT in molar ratios of 1/800, 1/400, 1/200, 1/100, 1/50, 1/25, 1/12.5 and 1/6.25 were prepared and subjected to capillary electrophoresis. The saturated curve showed the migration time of the AZT-RNA and AZT-DNA largely increased as the molar ratios of AZT/nucleotide (P) increased and became constant at low AZT contents (200 μM) [21,22]. In order to study the binding of AZT to RNA or DNA, Scatchard analysis [27,28] was

performed using data from increasing in the mobility shift of the AZT-RNA complexes. The generated curve is biphasic for drug-RNA complexes and two binding constants for AZT-RNA were estimated to be $K_1 = 7.30 \times 10^5$ M^{-1} and $K_2 = 1.90 \times 10^5$ M^{-1} [21].

Since the results from capillary electrophoresis showed two bindings for the AZT-RNA complexes, it is reasonable to assume (based on IR results) that the larger K value is due to the drug binding to the G bases, while the smaller K related to the AZT interaction with the U bases [23]. Similarly, electrophoresis results showed two bindings for AZT on DNA duplex with $K_1 = 2.60 \times 10^5$ M^{-1} and $K_2 = 1.20 \times 10^5$ M^{-1} [22]. The larger K is attributed to AZT binding to G-C base pair, while the smaller K can be related to drug interaction with A-T bases [22].

Molecular Modeling

Molecular modeling experiments were also performed in attempt to better understand the AZT-RNA and AZT-DNA binding modes. Energetically favorable models of the AZT-RNA and AZT-DNA complexes were built using the systematic procedure as described in the methods section, involving molecular modeling and docking followed by detailed molecular dynamic simulations. The energy of interaction (E_{int}) between the RNA or DNA and AZT molecule in a complex was calculated as a measure of stability of that complex. The lowest value of E_{int} obtained for AZT-DNA and AZT-RNA complexes was -20.94 kcal mol^{-1}, indicating that, energetically, this complex is the most stable (Fig. 1).

The suggested model shown in Fig. 1 implied that AZT binds guanine and uracil bases with minor perturbations of the backbone phosphate group. Guanine N2-H, N3 and uracil O2 and thymine are accessible targets for drug-RNA and drug-DNA bindings. Such bindings are established through guanine N2-H and uracil O2 and thymine atoms with AZT polar groups (O17-H and O19-H, respectively). The complex is further stabilized by a hydrogen bond between N14-H atom of AZT with O2 atom of ribose ring (Fig. 1). Similar modeling was used to locate the biogenic polyamines in the major and minor grooves of B-DNA duplex [29]. Even though the major target of AZT drug is DNA in nucleos, major interactions of AZT with protein and enzyme are recently reported [30-32].
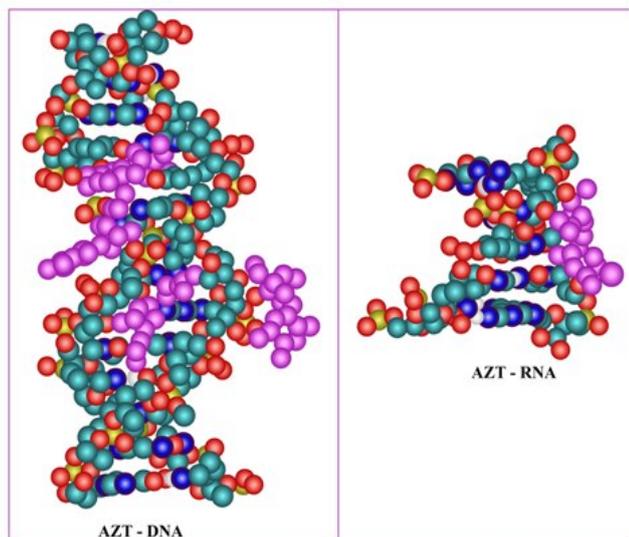
Fig. 1. Preferential binding model proposed for AZT-RNA and AZT-DNA interactions. Stick drawing (a) and the corresponding space-filling (b) models. AZT atoms are shown in violet color. H atoms have been omitted for clarity in both drawings. In both drawings, C, N, O and P atoms are cyan, blue, red and yellow, respectively.

SUMMARY

In conclusion, (a) AZT binds RNA and DNA through G-G, A-T and A-U base pairs with minor perturbations of the backbone phosphate group; (b) Two binding constants of $K_G = 7.3 \times 10^5$ M^{-1} and $K_U = 1.9 \times 10^5$ M^{-1} for AZT-RNA complexes and $K_G = 2.60 \times 10^5$ M^{-1} and $K_T = 1.20 \times 10^5$ M^{-1} for AZT-DNA adducts; (c) AZT interaction leads to no major alteration of A-RNA structure, while a major B to A conformational transition occurred for drug-DNA complexes; (d) Drug sugar pucker remains in C2′-endo/anti conformation and (e) Modeling study suggested that AZT interactions occur *via* hydrogen bonding to RNA or DNA duplex.

ACKNOWLEGMENTS

REFERENCES

[1] M. Rigourad, C. Ehresmann, M.A. Parniak, B. Ehresmann, R. Marquet. J. Biol. Chem. 277 (2002) 18611.

[2] C.C.J. Carpenter, D.A. Cooper, M.A. Fischl, J.M. Gatell, B.G. Gazzard, S.M. Hammer, M.S. Hirsch, D.M. Jacobsen, D.A. Katzenstein, J.S.G Montaner, D.D. Richman, M.S. Saag, M. Schechtler, R.T. Schooley, M.A. Thompson, S. Vella, P.G. Yeni, P.A. Volberding, J. Am. Med. Assoc. 283 (2000) 381.

[3] Center for Disease Control and Prevention HIV\AIDS Surveillance Report 11 (1999) 1-44.

[4] A. Bialkowska, K. Bailkowski, M. Gerschenson, B.A. Diwan, A.B. Jones, O.A. Olivero, M.C. Poirier, L.M. Anderson, K.S. Kasprzak, M.A. Sipowicz, Carcinogenesis 21 (2000) 1059.

[5] O.A. Olivero, M.K. Reddy, S.M. Pietras, M.C. Poirier, Exp. Biol. Med. 226 (2001) 446.

[6] Z. Zhang, B.A. Diwan, L.M. Anderson, D. Logsdon, O.A. Olivero, D.C. Haines, J.M. Rice, S.H. Yuspa, M.C. Poirier, Mol. Carcinog. 23 (1998) 45.

[7] M. Barile, D. Valenti, E. Quagliariello, S. Passarella, Gen. Pharm. 31 (1998) 531.

[8] M.G. Cid, I. Larripa, Mutat. Res. 321 (1994) 113.

[9] O.A. Olivero, F.A. Beland, M.C. Poirier, Int. J. Oncol. 4 (1994) 49.

[10] D.E. Gomez, A. Kassim, O.A. Olivero, Int. J. Oncol. 7 (1995) 1057.

[11] S. Alex, P. Dupuis, Inorg. Chim. Acta 157 (1989) 271.

[12] R. Ahmad, H. Arakawa, H.A. Tajmir-Riahi, Biophys. J. 84 (2003) 2460.

[13] HyperChem 7.0, 2002, Hypercube, Alberta. Canada.

[14] W.D. Cornell, R. Cieplak, C.L. Bayly, I.R. Gould, K.M. Merz, D.M. Ferguson, D.G. Spellmeyer, T. Fox, J.W. Caldwell, P.A. Kollman, J. Am. Chem. Soc. 117 (1995) 5179.

[15] A. Kamal, G. Ramesh, N. Laxman, P. Ramulu, O. Srinivas, K. Neelima, A.K. Kondapi, V.B. Sreenu, H.A. Nagarajaram, J. Med. Chem. 45 (2002) 4679.

[16] E.B. Starikov, M.A. Semenov, V.Y. Maleev, I.A. Gasan, Biopolymers 31 (1991) 255.

[17] B. Prescot, W. Steinmetz, G.J. Thomas, J.R.

Biopolymers 23 (1984) 235.

[18] D.M. Loprete, K.A. Hartman, Biochemistry 32 (1993) 4077.

[19] H. Arakawa, R. Ahmad, M. Naoui, H.A. Tajmir-Riahi, J. Biol. Chem. 275 (2000) 10150.

[20] E. Taillandier, J. Liquier, Methods Enzymol. 211 (1992) 307.

[21] A. Ahmed Ouameur, R. Marty, J.F. Neault, H.A. Tajmir-Riahi, DNA and Cell Biology 23 (2004) 783.

[22] R. Marty, A. Ahmed Ouameur, J.F. Neault, Sh. Nafisi, H.A. Tajmir-Riahi, DNA and Cell Biology 23 (2004) 139.

[23] S. Dijkstra, J.M. Benevides, G.J. Thomas JR, J. Mol. Struct. 242 (1991) 283.

[24] H.A. Tajmir-Riahi, J.F. Neault, M. Naoui, FEBS Lett. 370 (1995) 105.

[25] J.F. Neault, H.A. Tajmir-Riahi, Biophys. J. 76 (1999) 1776.

[26] H. Arakawa., J.F. Neault, H.A. Tajmir-Riahi, Biophys. J. 81 (2001) 1580.

[27] M.I. Klotz, L.D. Hunston, Biochemistry 10 (1973) 3065.

[28] M. I. Klotz, Science 217 (1982) 1247.

[29] A. Ahmed Ouameur, H.A. Tajmir-Riahi, J. Biol. Chem. 279 (2004) 42041.

[30] S. Gaudreau, J.F. Neault, H.A. Tajmir-Riahi, J. Biomol. Struct. Dyn. 19 (2002) 1007.

[31] S. Gaudreau, A. Novetta-Dellen, J.F. Neault, S. Diamantoglou, H.A. Tajmir-Riahi, Biopolymers (biospectroscopy) 72 (2003) 435.

[32] A. Ahmed Ouameur, J.F. Neault, S. Claveau, H.A. Tajmir-Riahi, Cell Biochem. Biophys. 42 (2005) 87